



OPEN

DATA DESCRIPTOR

The Mexican dataset of a repetitive transcranial magnetic stimulation clinical trial on cocaine use disorder patients: SUDMEX TMS

Diego Angeles-Valdez^{1,2}, Jalil Rasgado-Toledo¹, Viviana Villicaña³, Alan Davalos-Guzman⁴, Cristina Almanza¹, Alfonso Fajardo-Valdez¹, Ruth Alcala-Lozano⁴✉ & Eduardo A. Garza-Villarreal¹✉

Cocaine use disorder (CUD) is a global health problem with severe consequences, leading to behavioral, cognitive, and neurobiological disturbances. While consensus on treatments is still ongoing, repetitive transcranial magnetic stimulation (rTMS) has emerged as a promising approach for medication-resistant disorders, including substance use disorders. In this context, here we present the SUDMEX-TMS, a Mexican dataset from an rTMS clinical trial involving CUD patients. This longitudinal dataset comprises 54 CUD patients (including 8 females) with data collected at five time points: baseline (T0), two weeks (T1), three months (T2), six months (T3) follow-up, and twelve months (T4) follow-up. The clinical rTMS treatment followed a double-blinded randomized clinical trial design ($n = 24$ sham/30 active) for 2 weeks, followed by an open-label phase. The dataset includes demographic, clinical, and cognitive measures, as well as magnetic resonance imaging (MRI) data collected at all time points, encompassing structural (T1-weighted), functional (resting-state fMRI), and multishell diffusion-weighted (DWI-HARDI) sequences. This dataset offers the opportunity to investigate the impact of rTMS on CUD participants, considering clinical, cognitive, and multimodal MRI metrics in a longitudinal framework.

Background and Summary

Cocaine use disorder (CUD) is a worldwide public health problem with severe socio-economic consequences¹. Clinical outcomes include attention, learning, and working memory deficit, impulsivity, and structural brain alterations^{2,3}. Consequently, the pursuit of effective treatments has been a prominent focus in clinical research. Pharmacological approaches along with psychosocial therapy are currently the standard treatment with low to moderate efficacy⁴. Repetitive transcranial magnetic stimulation (rTMS) has emerged as an innovative therapeutic strategy for mitigating CUD symptoms and drug use⁵⁻⁷.

Current research is aiming towards affecting the circuits underpinning various addiction-related processes, including craving and impulsivity⁸. rTMS has the potential to activate these circuits and elicit long-term neuroplastic changes within the meso-cortico-limbic system⁹. Furthermore, the application of magnetic resonance imaging (MRI) has been instrumental in trying to find central biomarkers to measure disease severity and response to treatment.

Our dataset stems from our placebo-controlled double-blind randomized clinical trial (RCT) in which rTMS was used as an adjunct to standard treatment, referred to in this study as “treatment as usual” (TAU). The main advantage of our dataset is that we acquired longitudinal psychiatric interviews with standard clinical

¹Instituto de Neurobiología, Universidad Nacional Autónoma de México campus Juriquilla, Querétaro, Mexico.

²University of Groningen, Department of Biomedical Sciences of Cells and Systems, Cognitive Neuroscience Center, University Medical Center Groningen, Groningen, the Netherlands. ³Interdisciplinary Institute for Neuroscience, University of Bordeaux, CNRS UMR5297, 33000, Bordeaux, France. ⁴Laboratorio de Neuromodulación, Subdirección de Investigaciones Clínicas. Instituto Nacional de Psiquiatría Ramón de la Fuente Muñiz, Mexico City, Mexico.

✉e-mail: ruthalcalalozano@gmail.com; egarza@comunidad.unam.mx

	CUD Groups		Statistic
	Sham (n = 23)	Active (n = 30)	
Age			
	33.35 ± 8.15	36.07 ± 6.82	$t(42.61) = -1.29, p = 0.20$
Sex			
Male	20 (86.95%)	25 (83.33%)	$\chi^2(1) = 7.13e-32, p = 1$
Female	3 (13.05%)	5 (16.67%)	
Education in years			
	13.40 ± 2.83	12.90 ± 3.06	$t(49.09) = 0.60, p = 0.54$
Monthly Income, MXN			
	6591.30 ± 11386.63	5116.67 ± 6319.76	$t(32.25) = 0.55, p = 0.58$
Main substance of use			
Crack cocaine	20 (86.95%)	29 (96.6%)	$\chi^2(1) = 0.64, p = 0.42$
Cocaine	3 (13.05%)	1 (3.4%)	
Onset age of cocaine use			
	22.52 ± 6.76	22.77 ± 5.8	$t(43.38) = -0.13, p = 0.89$
Years of cocaine use			
	9.59 ± 7.61	12.07 ± 7.68	$t(47.70) = -1.17, p = 0.24$

Table 1. Demographic measures between groups. Continuous variables are reported as mean ± SD, and nominal as number (percentage from group): two-sample t-test and χ^2 was performed for each variable; no variables, n.a.: not applicable; CUD: cocaine use disorder.

assessment and multimodal MRI sequences, including multi-shell diffusion-weighted imaging. For specifics on the MRI sequences obtained, please refer to the participant's checklist available in the supplementary materials.

To date, our dataset has been used in various studies by other research teams. It has been employed to investigate both short and long-term clinical benefits of rTMS and their effects on functional connectivity¹⁰, to identify cognitive deficits in CUD participants through machine learning algorithms¹¹, to improve diffusion MRI segmentation methods via deep learning techniques¹², to predict clinical outcomes by examining microstructural changes¹³, and to establish a generalizable functional connectivity signature characterizing brain dysfunction in cocaine use disorder¹⁴. The publications and pre-prints mentioned represent just a portion of the possible applications of our data. In this release, we provide access to the complete dataset, encompassing clinical, cognitive, and MRI data, for further analysis. Previously, we have released another dataset, the SUDMEX-CONN¹⁵, which are independent yet acquired using the same scanner and similar sequences. Altogether, this dataset offers the opportunity to explore the longitudinal impact of rTMS as a promising adjunctive treatment for CUD and other SUDs, and to test new neuroimaging algorithms and analysis techniques. Some measurements from MRI and clinical tests have been used in different studies (See supplementary tables).

Methods

Participants. From a sample of $n = 117$ patients, 54 patients were included in the study. The reasons for the dropouts are in Supplementary Material. The study ran from May 2017 to September 2019. The study was conducted at the Clinical Research Division of the National Institute of Psychiatry in Mexico City, Mexico. The study was approved by the Ethics Committee of the Instituto Nacional de Psiquiatría “Ramón de la Fuente Muñiz” (INPRFM) (CEI/C/070/2016) and is in accordance with the latest version of the Declaration of Helsinki. The trial was registered at ClinicalTrials.gov (NCT02986438). All study participants were first interviewed to check for inclusion or exclusion criteria. Then, the patients were interviewed by the study psychiatrist, where she explained everything about the study in simple terms and followed the informed consent structure point by point. The patients were told about the absolute contraindications and possible secondary effects of the treatment, as well as how their data will be managed and disseminated. They were also told to bring a family member or another person to explain and co-sign the consent if they felt they had any doubts about it, or they could opt-out from the study without consequences at this or any point until their understanding was ensured. Patients were not paid for their participation. The patients who signed the informed consent were then included in the study. Cocaine dependence was diagnosed in CUD patients using the MINI International Neuropsychiatric Interview-Plus Spanish version 5.0.0¹⁶. Demographic characteristics between groups are summarized in Table 1.

Experimental design. The study consisted of four stages: 1) a screening interview to confirm substance use disorder (SUD) diagnosis by a trained psychiatrist; 2) participants underwent a full clinical evaluation and initial MRI acquisition at baseline or Time 0 (T0); 3) an Acute stage (RCT) where patients underwent regularly scheduled sessions (Active or Sham rTMS) for 10 days over 2 weeks, after which they underwent clinical evaluation and MRI acquisition called Time 1 or T1. The blinding was opened, and only the patients in the sham group were invited to initiate active rTMS treatment for 2 weeks, after which they underwent another clinical evaluation and MRI acquisition called Time 1–4 or T1–4 (4 as in 4 weeks time). 4) Finally, after active rTMS treatment, all patients went into the open-label maintenance phase, and they underwent clinical evaluation and MRI acquisition at three months (Time 2 or T2), six months (Time 3 or T3) and 12 months (Time 4 or T4). The study design is detailed in Fig. 1.

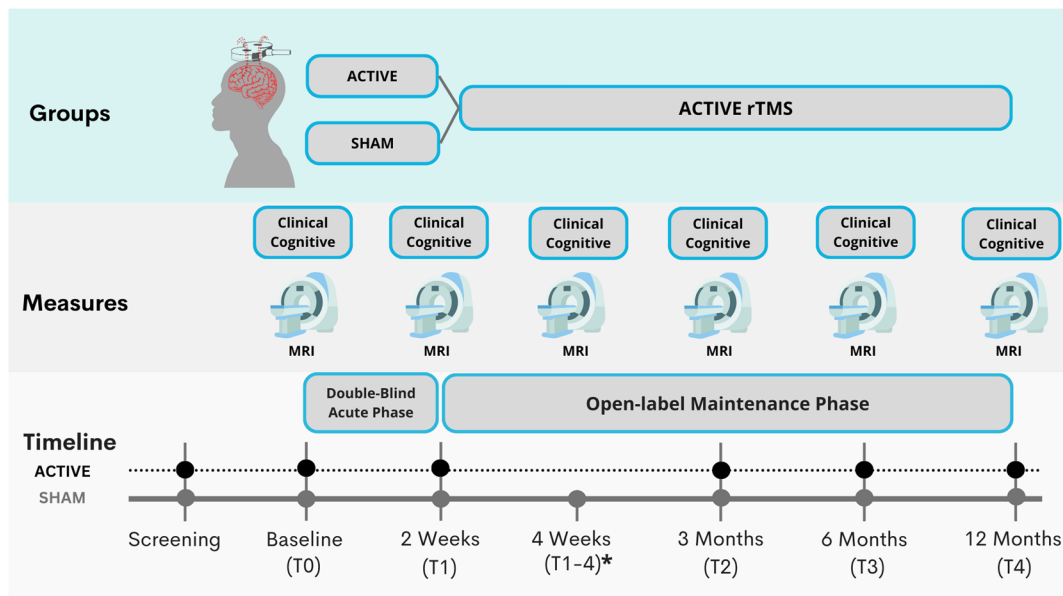


Fig. 1 SUDMEX-TMS experimental design. Clinical and MRI data were collected at the time of baseline (T0), at two weeks (T1), three months (T2), six months (T3) and 12 months (T4); * Patients who received the sham treatment and then received active treatment (T1–4).

Study dropout. Out of the 54 recruited patients (T0), 30 were randomly assigned to active treatment, and 24 to sham rTMS. Five patients in the active rTMS group and four in the sham group discontinued the study, resulting in 24 patients completing the double-blind acute phase (2 weeks) in the active group and 20 in the sham group. Following this phase, 14 patients from the sham group chose to receive 2 weeks of acute rTMS therapy (2 weeks) after the sham phase. Participants dropouts were as follows: 1) 20 patients underwent 3 months of twice-weekly rTMS sessions, with 15 initially assigned to the active group and 5 to the sham group (T2); 2) among the study participants, 15 patients (n = 10 active, 5 sham), successfully completed 6 months of rTMS sessions (T3); and 3) 7 patients (n = 4 active, 3 sham), successfully completed 12 months of bi-weekly rTMS sessions (T4). Due to significant attrition at T1 (2 weeks), when the study was only about 30% complete, we extended the maintenance phase to 6 months instead of 12 months for new participants after obtaining approval from the ethics committee. Importantly, no adverse effects related to rTMS treatment were reported by patients who discontinued participation at any stage. None of the patients who discontinued treatment at any point reported adverse effects from rTMS.

Study timeline. At Visit 1, the patients arrived for a clinical screening interview to confirm they met the criteria. At Visit 2, enrolled patients underwent a full clinical assessment (Time 0 or T0). Initial MRI scanning occurred at Visit 3 (Baseline or MRI-T0). The clinical interview preceded MRI acquisition and always occurred within 3 days. Following MRI acquisition, we initiated the double-blind rTMS/sham acute phase (see below). Patients underwent regularly scheduled sessions (Active or Sham rTMS) for 10 days over 2 weeks. At the conclusion of 2 weeks (Visit 4; T1), they underwent clinical assessment and repeated MRI scanning, marking the end of the acute phase and the start of the open-label maintenance phase. The blind (Active vs. Sham) was decoded for each participant at the end of their acute phase. Patients assigned to Active rTMS entered the maintenance phase directly after T1. Patients assigned to Sham rTMS were given the choice to leave the study or continue with active open-label rTMS for compassionate use. Patients assigned to the Sham group who agreed to continue, received 2-weeks (10 days) acute treatment before continuing to the maintenance phase. The maintenance phase was initially designed to include 2 weekly rTMS sessions and clinical assessments and MRI scans at 3 months, 6 months and 12 months. However, the maintenance phase was subsequently changed to 3 months for new enrollments.

Magnetic resonance imaging acquisition. MRI sequences were acquired using a Philips Ingenia 3T MR system (Philips Healthcare, Best, The Netherlands, and Boston, MA, USA), with a 32-channel dS Head coil. The order of the sequences was the following for the single session: 1) resting state (rs-fMRI), 2) T1-weighted (T1w), and 3) High Angular Resolution Diffusion Imaging (DWI-HARDI). This order was maintained across participants. Before the MRI acquisition, the amount of alcohol in participants' blood was measured using a breathalyzer alcohol test, and other substances were measured using a breath alcohol test and *Instant-view*TM multi-drug urine test. The total scan time was approximately 50 min. During the study, the participants were fitted with MRI-compatible headphones and goggles (see Table 2). Anonymization of the dataset was performed using pydeface to remove facial features¹⁷.

Anatomical images. T1-weighted images were acquired using a 3D FFE SENSE sequence, TR/ TE = 7/3.5 ms, FOV = 240 mm², matrix = 240 × 240 mm, 180 slices, gap = 0, plane = Sagittal, voxel = 1 × 1 × 1 mm (5 participants were acquired with a voxel size = 0.75 × 0.75 × 1 mm).

Acquisitions		
Clinical measures	Cognitive measures	MRI sequences
<ul style="list-style-type: none"> Instant-view urine test MINI-Plus ASI SCID-II SCL-R Revised CCQ General & CCQ Now WHODAS BIS-11 EHI short HDRS HARS PSQI VAS 	<ul style="list-style-type: none"> Berg's Card Sorting Test Flanker task Go/No-go task Letter number sequencing Digit span backward Iowa gambling task Tower of London Reading mind in the eyes 	<ul style="list-style-type: none"> rs-fMRI (T2*) Structural scan (T1-weighted) High Angular Resolution Diffusion Imaging (DWI)

Table 2. Summary of the acquired data for clinical measures, cognitive measures and MRI sequences. Mini International Neuropsychiatric Interview - Plus; MINI- Plus, Addiction Severity Index; ASI, Structured Clinical Interview for DSM-IV Axis II Personality Disorders; SCID-II, Symptom Checklist-90-Revised; SCL-R, Cocaine Craving Questionnaire General CCQ-G and Now CCQ-N, World Health Organization Disability Assessment Schedule 2.0; WHODAS, Barratt Impulsiveness Scale v. 11; BIS-11, Edinburgh Handedness Inventory Short Form; EHI short, Hamilton Depression Rating Scale (HDRS), Hamilton Anxiety Rating Scale (HARS), Pittsburgh Sleep Quality Index (PSQI), and Cocaine Craving visual analogue scale (VAS).

Diffusion-weighted imaging. The DWI-HARDI was a spin echo (SE) sequence, with TR/TE = 9000/127 ms, FOV = 230 mm² (for 4 participants = 224mm²), matrix = 96 × 96 (the first 4 participants = 112 × 112), number of slices = 57 (for 4 participants = 58), gap = 0, plane = axial, voxel = 2.4 × 2.4 × 2.5 mm (the first 4 participants = 2 × 2 × 2.3 mm), directions: b₀ = 8, b-value 1000 = 32 s/mm², b-value 2500 = 96 s/mm² (for 4 participants: 96 = b-value 3,000 s/mm²), with a total of 136 directions. We acquired a DWI-HARDI with an opposite direction for field mappings using a SE EPI sequence with the following parameters: TR/TE = 9000/127 ms, flip angle = 90°, matrix = 128 × 128 (the first 4 participants = 112 × 112), voxel size = 1.8 × 1.8 × 2.5 mm (for 4 participants = 2 × 2 × 2.3 mm), directions: b₀ = 7, number of slices = 57 (for first 4 participants = 58), phase encoding direction = PA.

Resting-state functional MRI. Resting-state fMRI sequences were acquired using a gradient recalled (GE) echo planar imaging (EPI) sequence with the following parameters: dummies = 5, repetition time (TR)/echo time (TE) = 2000/30.001 ms, flip angle = 75°, matrix = 80 × 80, field of view = 240mm², voxel size = 3 × 3 × 3.33 mm, gap = 0, slice acquisition order = interleaved (ascending), number of slices = 36, phase encoding direction = AP. The total scan time of the rs-fMRI session was 10 min, with a total of 300 volumes acquired. All participants were instructed to keep their eyes open, and to relax while not thinking about anything in particular. We used MRI-compatible goggles (fiber optic glasses SV-7021, Avotec) to show the participants a fixation cross (white cross with black background), and we used the included eye-tracking camera to prevent participants from falling asleep during this sequence. If the participants closed their eyes for more than 10 seconds, we would wake them up using the communication through the headphones, reminding them to try to not fall asleep for the 10 minutes the sequence lasted, and we restarted the sequence over. We acquired an opposite direction sequence for field mapping, using the same GE-EPI sequence with the following parameters: TR/TE = 2000/30 ms, flip angle = 75°, matrix = 80 × 80, voxel size = 3 × 3 × 3mm, number of slices = 36, volumes = 4, phase encoding direction = PA.

Transcranial magnetic stimulation. We performed a placebo-controlled double-blind randomized controlled trial (RCT) with parallel groups (Sham/Active) for 2 weeks (acute phase) and an open-label maintenance phase for 6 months. For the acute phase, we used a MagPro R301 Option magnetic stimulator and a figure-of-eight B65-A/P coil (MagVenture, Alpharetta, GA); for the maintenance phase, we used a MagPro R30 stimulator and a figure-of-eight MCF-B70 coil (MagVenture). The acute phase comprised 10 weekdays of 5,000 pulses per day (two sessions of 50 trains at 5 Hz, 50 pulses/train, 10 s inter-train interval, and 15 min inter-session interval). The maintenance phase comprised 3 and 6 months of 5,000 pulses per day, 2 sessions per week. The maintenance phase comprised two 5-Hz excitatory frequency (5000 pulses per day) sessions per week. The stimulation was delivered at 100% motor threshold to the left Dorso-Lateral Prefrontal Cortex (IDLDFC). The motor threshold was determined in each patient as described by Rossini *et al.*¹⁸. We used a vitamin E capsule as a fiducial during MRI acquisition to identify the stimulation cortical target due to a lack of a brain navigator. In all rTMS sessions, we used either the 5.5 cm anatomic Rule or the Beam F3 method. We changed to the superior Beam F3 method after the first 16 participants to improve IDLDFC localization¹⁹. The motor threshold was maintained at 100% in all patients. Electrodes were applied to all patient's left temporalis muscles to simulate muscular contraction in the sham group, enhancing the sham and blinding. More information about TMS procedures is available in the supplementary material.

Clinical measures. Patients underwent paper-based clinical tests during each session. The included assessments were: 1) Hamilton Anxiety Rating Scale (HARS), 2) Mini International Neuropsychiatric Interview - Plus (MINI-Plus), 3) Pittsburgh Sleep Quality Index (PSQI), 4) Cocaine Craving visual analog scale (VAS), 5) Addiction Severity Index (ASI), 6) Structured Clinical Interview for DSM-IV Axis II Personality Disorders (SCID-II), 7) Symptom Checklist-90-Revised (SCL-R), 8) Cocaine Craving Questionnaire General (CCQ-G)

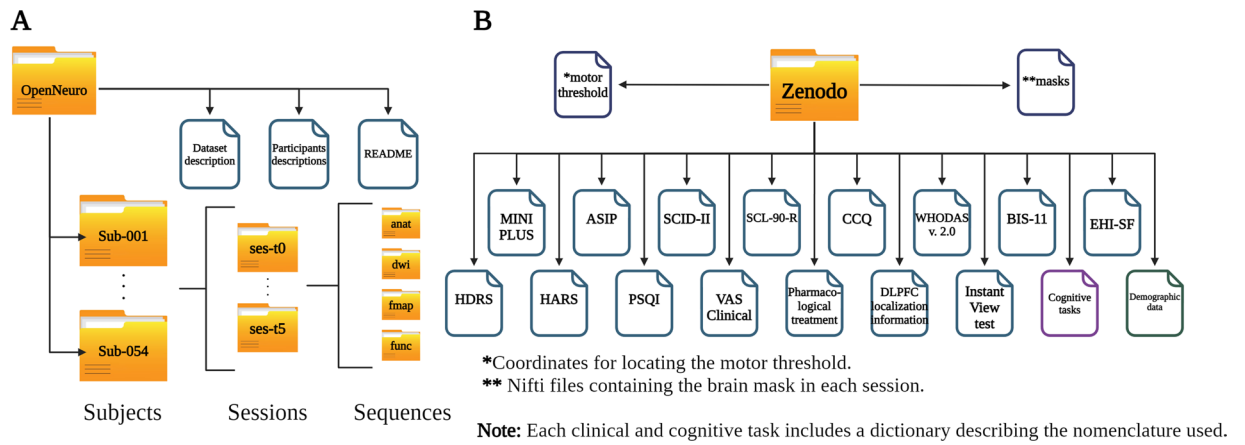


Fig. 2 Descriptive image of the existing files in each platform. **(A)** MRI data files and BIDs organization in OpenNeuro platform, **(B)** Clinical and cognitive files and organization in Zenodo platform.

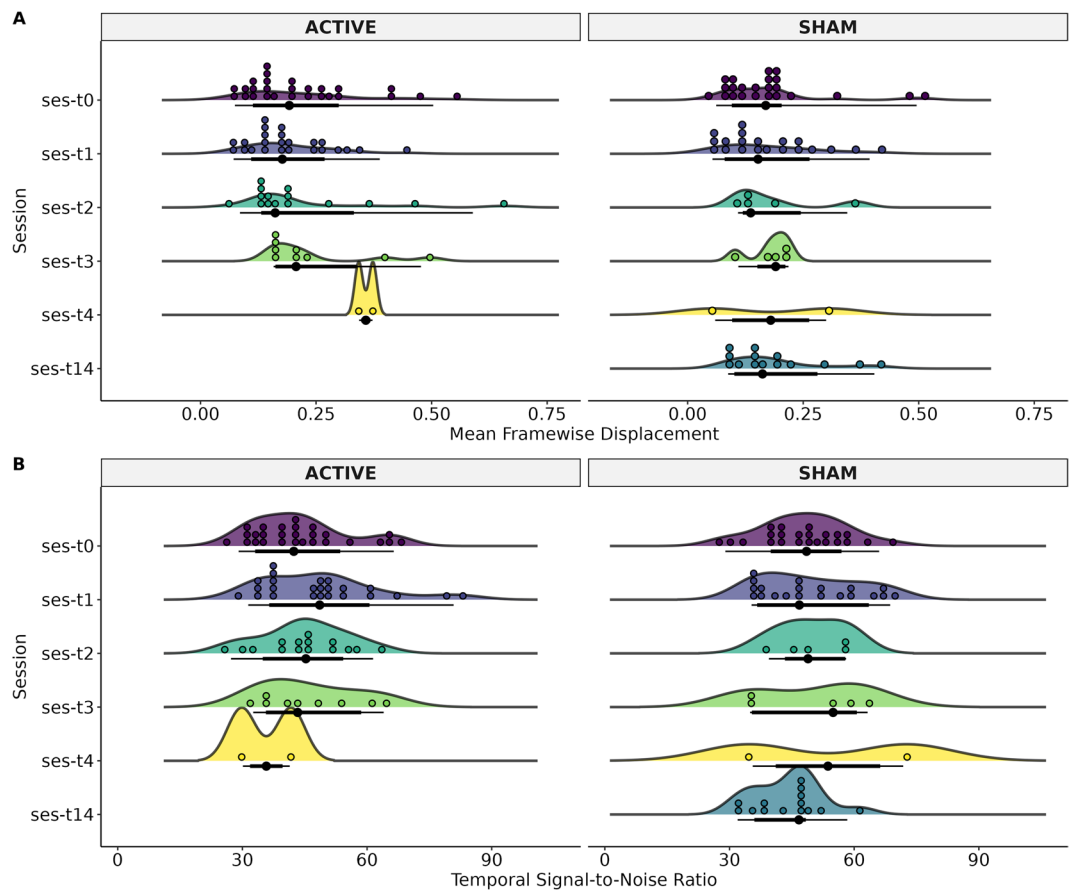


Fig. 3 Status of the structural weighted image of each MRI-Session (ses): baseline (T0), at two weeks (T1), three months (T2), and six months (T3), and patients that had 12 months (T4). The T14 time was for patients in the Sham group who decided to continue the clinical trial with open-label rTMS. The T14 refers to 2 weeks after T1 (4 weeks after T0). **(A)** Signal-to-Noise Ratio (SNR), and **(B)** Contrast-to-Noise Ratio (CNR).

and Now (CCQ-N), 9) World Health Organization Disability Assessment Schedule 2.0 (WHODAS), 10) Barratt Impulsiveness Scale v. 11 (BIS-11), 11) Edinburgh Handedness Inventory Short Form, 12) Hamilton Depression Rating Scale (HDRS). Trained mental health psychologists and psychiatrists conducted these tests in a distraction-free environment. A summary of the acquired data is presented in Table 2. In this section, we present a selection of the metrics employed in this study. For a comprehensive description of the remaining metrics, please refer to Angeles-Valdez *et al.*¹⁵ and the original publications associated with each measure.

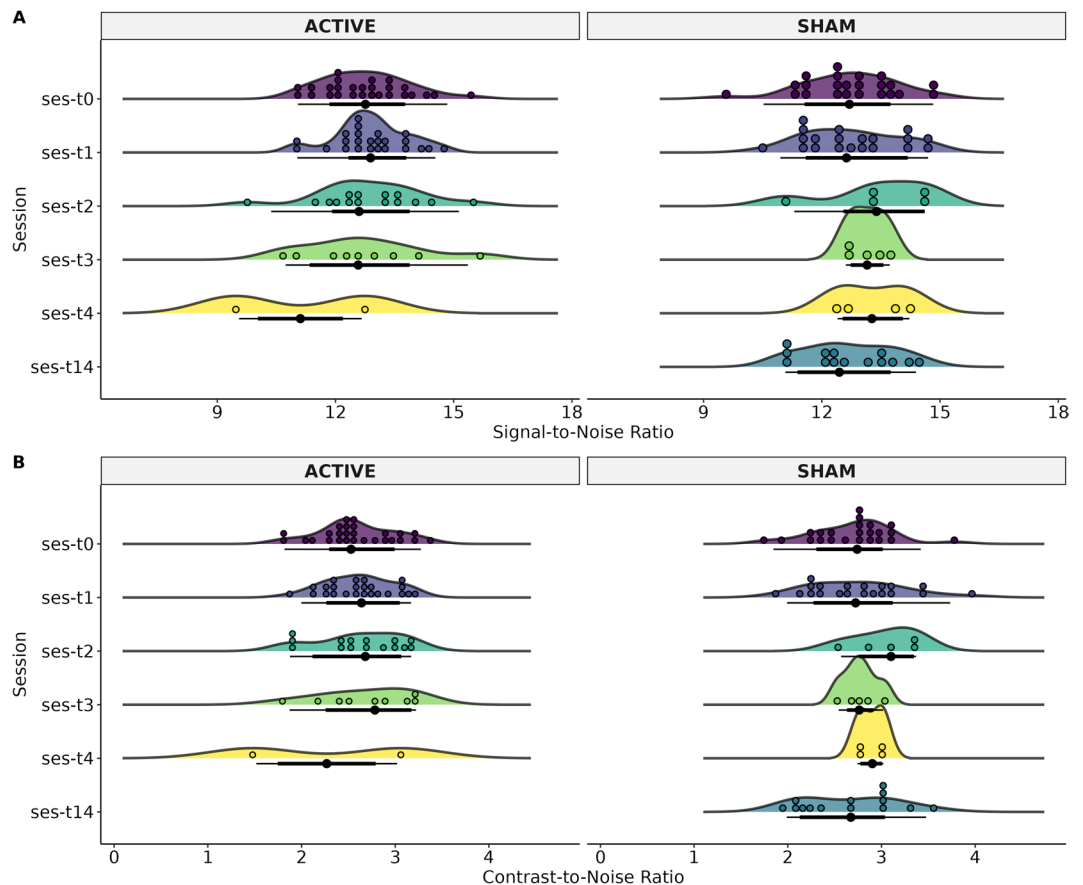


Fig. 4 Status of the resting-state image of each MRI-Session (ses): baseline (T0), at two weeks (T1), three months (T2), and six months (T3), and patients that had 12 months (T4). The T14 time was for patients in the Sham group who decided to continue the clinical trial with open-label rTMS. The T14 refers to 2 weeks after T1 (4 weeks after T0). **(A)** Mean Framewise Displacement (FD) and, **(B)** Temporal Signal-to-Noise Ratio (tSNR).

Hamilton Anxiety Rating Scale (HARS). The Hamilton Anxiety Rating Scale (HAM-A) assesses the global severity of anxiety and is valuable for monitoring treatment response²⁰. It comprises 14 items, measuring 13 anxious signs and symptoms, with the last item evaluating the patient's behavior during the interview. Each item is scored from 0 to 4 points, considering both intensity and frequency. The total score is the sum of each item's score, ranging from 0 to 56 points. Optimal HAM-A score ranges are as follows: no/minimal anxiety (≤ 7), mild anxiety (8–14), moderate anxiety (15–23), and severe anxiety (≥ 24).

Pittsburgh Sleep Quality Index (PSQI). This instrument was developed to measure sleep quality in patients with psychiatric disorders²¹. It consists of 24 items, the assessment encompasses 7 dimensions: Subjective sleep quality, Sleep latency, Duration of sleep, Usual sleep efficiency, Sleep disturbances, Use of medication, and Daytime dysfunction. Respondents use a Likert-type scale ranging from 0 to 4. The correction involves obtaining a sleep profile for each dimension, ranging from 0 to 3, and a total score that can range from 0 to 21.

Cocaine Craving visual analogue scale (VAS). This instrument is designed for the subjective assessment of the participant's current craving. The visual scale comprises a continuous line of 10 cm (including 2 decimal places). The left end represents 'no craving,' and the right end represents 'the most intense craving.' Participants are instructed to mark the intensity of their current craving by placing a cross on the scale²².

Hamilton Depression Rating Scale (HDRS). The Hamilton Rating Scale for Depression was employed to gauge the severity of depression²³. The version we used is one of 17 items, with its content centering on depressive behavior. Vegetative, cognitive, and anxiety symptoms carry the most significant weight in the total calculation of the scale. Cutoff points for defining severity are as follows: no depression (0–7), mild depression (8–16), moderate depression (17–23), and severe depression (≥ 24).

Cognitive tests. At each of the three stages, patients underwent a comprehensive neuropsychological assessment. The computer-based assessments, including Berg's Card Sorting Test, Flanker Task, Go/No-Go task, Iowa Gambling Task, Tower of London, and Reading the Mind in the Eyes Test, were conducted using the Psychology Experiment Building Language (PEBL) version 2.0 with Spanish translation²⁴. On the other hand, the Digit-Span Backward and Letter-Numbers Sequencing exams were administered on paper. All cognitive tests

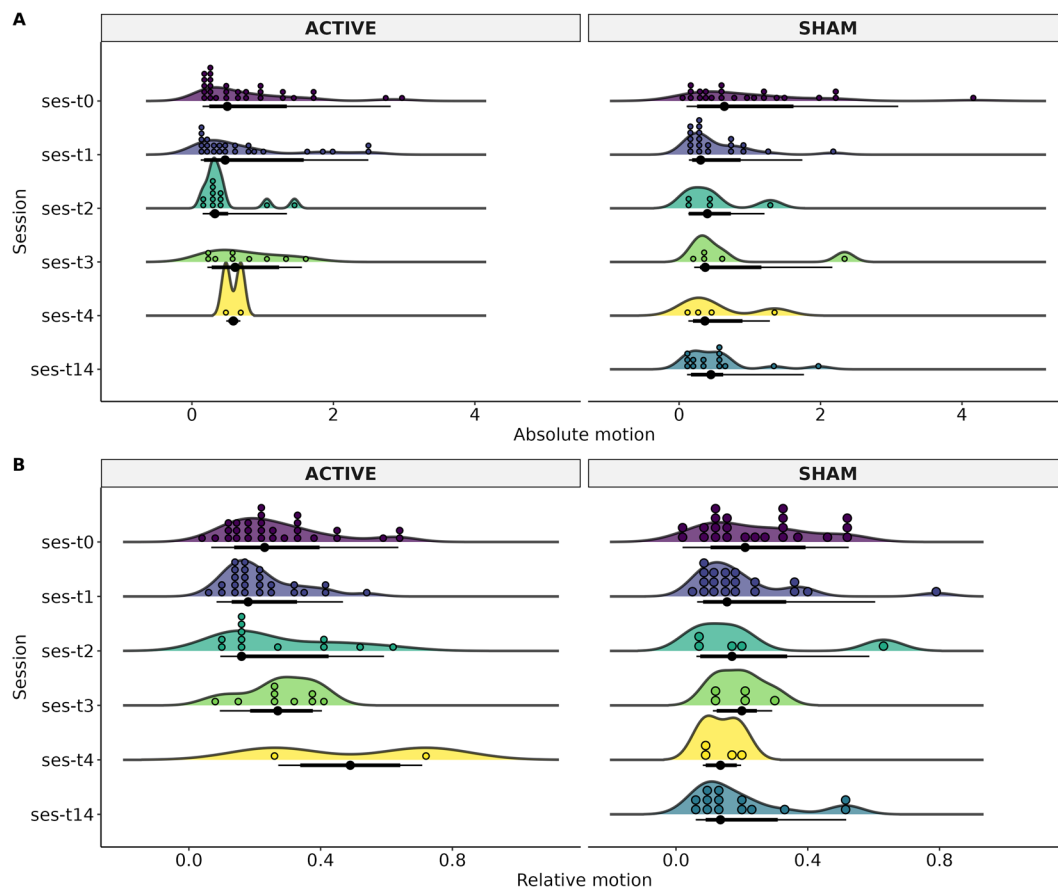


Fig. 5 Participant motion of the diffusion-weighted image of each MRI-Session (ses): baseline (T0), at two weeks (T1), three months (T2), and six months (T3), and patients that had 12 months (T4). The T14 time was for patients in the Sham group who decided to continue the clinical trial with open-label rTMS. The T14 refers to 2 weeks after T1 (4 weeks after T0). (A) Absolute motion, (B) Relative motion.

were administered by a licensed psychologist in a quiet setting to minimize distractions. The assessments took place after the MRI scan, with a total duration of 45 minutes per participant.

Here, we only describe some of the metrics applied, the complete descriptions of the rest of the metrics can be found in the work by Angeles-Valdez *et al.*¹⁵, as well as in the original publications for each measure.

Data Records

MRI organization. The organization of the dataset follows the Brain Imaging Data Structure (BIDS, v. 1.0.1) (<https://bids-specification.readthedocs.io/>), commonly used to facilitate data sharing and project unifications by folder and file name structure according to sequence modality (Fig. 2A)²⁵. MRI images are shared in the Neuroimaging Informatics Technology Initiative (Nifti) format converted from Digital Imaging and Communication In Medicine (DICOM) using dcm2bids v.2.1.4²⁶, along with data descriptions and metadata in JavaScript Object Notification files. The dataset is available and hosted on the OpenNeuro²⁷ Data sharing platform (<https://openneuro.org/datasets/ds003037/versions/2.1.0>)²⁸. The Brain Imaging Data Structure (BIDS) employs a hierarchical subdirectory layout. At the root resides the dataset, followed by individual session folders. Within each session, modality-specific folders organize the sequences. The MRI images are inside each folder alongside a JSON descriptor, detailing its run-specific metadata (Fig. 2A). The structure tutorial is available on the BIDS website (<https://bids-specification.readthedocs.io>).

Clinical and cognitive organization. The clinical, cognitive, and demographic data are available in the Zenodo repository (<https://doi.org/10.5281/zenodo.10409461>)²⁹. The data set is curated and organized by test type for each experimental phase. The Zenodo repository houses each test type in an individual spreadsheet, separated by variables (columns) and each participants' observations (rows), with individual items and total scores as variables. Additionally, a dedicated metadata sheet acts as a comprehensive glossary that defines each variable's nomenclature, type, and level of measurement (Fig. 2B).

Technical Validation of the MRI

Quality Control. To assess the quality control of sMRI and rsMRI sequences we used the MRIQC v.0.15 tool³⁰. The extracted values for sMRI were Signal-to-Noise Ratio (SNR) and Contrast-to-Noise Ratio (CNR) (Fig. 3). SNR is related to the ratio of the mean voxel intensity of an image in contrast with the random noise intensity³¹, whereas the CNR measure is an extension of SNR that is not influenced by contrast changes³².

For rsMRI the extracted values were Framewise Displacement (FD) and temporal Signal-to-Noise Ratio (tSNR) (Fig. 4). FD is the sum of parameters of translational and rotational realignment of head motion^{32,33}, while tSNR is calculated as the division of the mean of the time series by its standard deviation, when spatial resolution increases, tSNR decreases³⁴.

For Diffusion-weighted images, we performed automated diffusion MRI QC (FSL EDDY_QC) to extract QC metrics sensitive and specific to artifacts³⁵, at a single level. The extracted values were related to motion: absolute (motion referenced to the middle time-point) and relative (motion compared with the previous time-point). The automated QC tool relies on EDDY³⁶, used to calculate the motion of dMRI data through volume-to-volume motion based on 6 parameters of the degree of freedom (Fig. 5).

Usage Notes

The present dataset consists of cocaine use disorder patients treated using rTMS therapy followed up to 12 months and divided into a sham group and an active rTMS group for the first 2 weeks. New studies can be focused on the impact of rTMS over the active group in contrast to sham, on multimodal MRI data and/or clinical/cognitive measures. To use the present dataset in conjunction with other datasets, such as those of the ENIGMA consortium, we recommend the use of an MRI-site harmonization technique such as ComBatHarmonization³⁷. Here, we provided QC information in order to facilitate data usage of which participants could be dismissed from data analysis. We recommend the use of artifact correction methods for preprocessing data due to the high motion of some subjects during scanning. The present dataset was released and peer reviewed in 2023 based on MRI OpenNeuro version 2.1.0 and Zenodo platform version 4.2.

Code availability

The MRI dataset can be found in <https://openneuro.org/datasets/ds003037/versions/2.1.0>²⁸. Please download the latest available version as there may be updates. Clinical and cognitive data are available in Zenodo <https://doi.org/10.5281/zenodo.10409461>²⁹. No custom code was used in this work.

Received: 31 July 2023; Accepted: 9 April 2024;

Published online: 22 April 2024

References

1. Peacock, A. *et al.* Global statistics on alcohol, tobacco and illicit drug use: 2017 status report. *Addiction* **113**, 1905–1926 (2018).
2. Potvin, S., Stavro, K., Rizkallah, E. & Pelletier, J. Cocaine and cognition: a systematic quantitative review. *J. Addict. Med.* **8**, 368–376 (2014).
3. Fryer, R. G. Jr, Heaton, P. S., Levitt, S. D. & Murphy, K. M. Measuring crack cocaine and its impact. *Econ. Inq.* **51**, 1651–1681 (2013).
4. Kampman, K. M. The treatment of cocaine use disorder. *Sci Adv* **5**, eaax1532 (2019).
5. Terraneo, A. *et al.* Transcranial magnetic stimulation of dorsolateral prefrontal cortex reduces cocaine use: A pilot study. *Eur. Neuropsychopharmacol.* **26**, 37–44 (2016).
6. Politi, E., Fauci, E., Santoro, A. & Smeraldi, E. Daily sessions of transcranial magnetic stimulation to the left prefrontal cortex gradually reduce cocaine craving. *Am. J. Addict.* **17**, 345–346 (2008).
7. Protasio, M. I. B. *et al.* The Effects of Repetitive Transcranial Magnetic Stimulation in Reducing Cocaine Craving and Use. *Addictive Disorders & Their Treatment* **18**, 212–222 (2019).
8. Steele, V. R. & Maxwell, A. M. Treating cocaine and opioid use disorder with transcranial magnetic stimulation: A path forward. *Pharmacol. Biochem. Behav.* **209**, 173240 (2021).
9. Moretti, J., Poh, E. Z. & Rodger, J. rTMS-Induced Changes in Glutamatergic and Dopaminergic Systems: Relevance to Cocaine and Methamphetamine Use Disorders. *Frontiers in Neuroscience*. **14**, 137 (2020).
10. Garza-Villarreal, E. A. *et al.* Clinical and Functional Connectivity Outcomes of 5-Hz Repetitive Transcranial Magnetic Stimulation as an Add-on Treatment in Cocaine Use Disorder: A Double-Blind Randomized Controlled Trial. *Biological Psychiatry: Cognitive Neuroscience and Neuroimaging*. **6**, 745–757 (2021).
11. Jiménez, S. *et al.* Identifying cognitive deficits in cocaine dependence using standard tests and machine learning. *Prog. Neuropsychopharmacol. Biol. Psychiatry* **95**, 109709 (2019).
12. Zhang, F. *et al.* Deep learning based segmentation of brain tissue from diffusion MRI. *Neuroimage* **233**, 117934 (2021).
13. Rasgado-Toledo, J., Issa-García, V., Alcalá-Lozano, R., Garza-Villarreal, E. A. & González-Escamilla, G. Cortical and subcortical microstructure integrity changes after repetitive transcranial magnetic stimulation therapy in cocaine use disorder and relates to clinical outcomes. *Addict. Biol.* **29**, e13381 (2024).
14. Zhao, K. *et al.* A generalizable functional connectivity signature characterizes brain dysfunction and links to rTMS treatment response in cocaine use disorder. *medRxiv*, <https://doi.org/10.1101/2023.04.21.23288948> (2023).
15. Angeles-Valdez, D. *et al.* The Mexican magnetic resonance imaging dataset of patients with cocaine use disorder: SUDMEX CONN. *Sci Data* **9**, 133 (2022).
16. Ferrando, L., Bobes, J., Gibert, M., Soto, M. & Soto, O. M.I.N.I. Mini International Neuropsychiatric Interview. Versión en español 5.0.0.DSM-IV. Instituto IAP, Madrid, (1998).
17. Gulban, O. F. *et al.* poldracklab/pydeface: v2. 0.0. Zenodo <https://doi.org/10.5281/zenodo.3524401> (2019).
18. Rossini, P. M. *et al.* Non-invasive electrical and magnetic stimulation of the brain, spinal cord and roots: basic principles and procedures for routine clinical application. Report of an IFCN committee. *Electroencephalogr. Clin. Neurophysiol.* **91**, 79–92 (1994).
19. Trapp, N. T. *et al.* Reliability of targeting methods in TMS for depression: Beam F3 vs. 5.5 cm. *Brain Stimul.* **13**, 578–581 (2020).
20. Hamilton, M. The assessment of anxiety states by rating. *Br. J. Med. Psychol.* **32**, 50–55 (1959).
21. Buysse, D. J. *et al.* The Pittsburgh Sleep Quality Index: a new instrument for psychiatric practice and research. *Psychiatry Res.* **28**, 193–213 (1989).
22. Nicholson, A. N. Visual analogue scales and drug effects in man. *Br. J. Clin. Pharmacol.* **6**, 3–4 (1978).
23. Ramos-Brieva, J. A. & Cordero Villafáfila, A. [Relation between the validity and reliability of the Castilian version of the Hamilton Rating Scale for Depression]. *Actas Luso. Esp. Neurol. Psiquiatr. Cienc. Afines* **14**, 335–338 (1986).
24. The Psychology Experiment Building Language (PEBL) and PEBL Test Battery. *J. Neurosci. Methods* **222**, 250–259 (2014).
25. Gorgolewski, K. J. *et al.* The brain imaging data structure, a format for organizing and describing outputs of neuroimaging experiments. *Sci Data* **3**, 160044 (2016).
26. Li, X., Morgan, P. S., Ashburner, J., Smith, J. & Rorden, C. The first step for neuroimaging data analysis: DICOM to NIFTI conversion. *J. Neurosci. Methods* **264**, 47–56 (2016).
27. Markiewicz, C. J. *et al.* The OpenNeuro resource for sharing of neuroscience data. *Elife* **10**, (2021).

28. Angeles-Valdez, D. *et al.* SUDMEX_TMS. *OpenNeuro* <https://doi.org/10.18112/openneuro.ds003037.v2.1.0> (2023).
29. Angeles-Valdez, D. *et al.* The Mexican dataset of an rTMS clinical trial on cocaine use disorder patients: SUDMEX TMS (V4.2). *Zenodo*. <https://doi.org/10.5281/zenodo.10409461> (2023).
30. Esteban, O. *et al.* MRIQC: Advancing the automatic prediction of image quality in MRI from unseen sites. *PLoS One* **12**, e0184661 (2017).
31. McRobbie, D. W., Moore, E. A., Graves, M. J. & Prince, M. R. *MRI from Picture to Proton*. (Cambridge University Press, 2017).
32. Magnotta, V. A., Friedman, L. & Birn, First Measurement of Signal-to-Noise and Contrast-to-Noise in the fBIRN Multicenter Imaging Study. *J. Digit. Imaging* **19**, 140–147 (2006).
33. Power, J. D., Barnes, K. A., Snyder, A. Z., Schlaggar, B. L. & Petersen, S. E. Spurious but systematic correlations in functional connectivity MRI networks arise from subject motion. *Neuroimage* **59**, 2142–2154 (2012).
34. Murphy, K., Bodurka, J. & Bandettini, P. A. How long to scan? The relationship between fMRI temporal signal to noise ratio and necessary scan duration. *Neuroimage* **34**, 565–574 (2007).
35. Bastiani, M. *et al.* Automated quality control for within and between studies diffusion MRI data using a non-parametric framework for movement and distortion correction. *Neuroimage* **184**, 801–812 (2019).
36. Andersson, J. L. R. & Sotiropoulos, S. N. An integrated approach to correction for off-resonance effects and subject movement in diffusion MR imaging. *Neuroimage* **125**, 1063–1078 (2016).
37. Fortin, J.-P. *et al.* Harmonization of cortical thickness measurements across scanners and sites. *Neuroimage* **167**, 104–120 (2018).

Acknowledgements

We thank the people who helped this project in one way or another: Ernesto Reyes-Zamorano, Francisco J. Pellicer Graham, Erik Morelos-Santana, Sarael Alcauter, Luis Concha, Bernd Foerster, Alejandra López-Castro and Josué Mendoza. We also thank Rocío Estrada Ordoñez and Isabel Lizariandari Espinosa Luna at the Unidad de Atención Toxicológica Xochimilco for all their help and effort. Finally, we thank the study participants for their cooperation and patience. This study was supported by public funds CONACYT FOSISS No. 0260971 and CONACYT No. 253072. Diego Angeles-Valdez is a doctoral student from Programa de Maestría y Doctorado en Psicología, Universidad Nacional Autónoma de México (UNAM) and received fellowship No. 1003596 from Consejo Nacional de Ciencia y Tecnología (CONACYT). Jalil Rasgado Toledo is a doctoral student from the Programa de Doctorado en Ciencias Biomédicas, Universidad Nacional Autónoma de México (UNAM), and received fellowship 858667 from CONACYT. This work received support from Luis Aguilar and Alejandro De León of the Laboratorio Nacional de Visualización Científica Avanzada, and also we appreciate the technical support by Leopoldo González-Santos.

Author contributions

E.G.V. originated the concept of the dataset, designed the study, provided funding, and acquired pilots. R.A.L., D.A.V., and V.V. recruited patients. D.A.V. and V.V. acquired the MRI data. D.A.V., and V.V. implemented the cognitive tests. R.A.L. implemented and managed the clinical part of the study. D.A.V., J.R.T., and C.A., performed the analysis and technical validation. D.A.V., J.R.T., A.F.V. and D.A.V., J.R.T., and E.G.V. created, reviewed, and approved the manuscript.

Competing interests

The authors declare no competing interests.

Additional information

Supplementary information The online version contains supplementary material available at <https://doi.org/10.1038/s41597-024-03242-y>.

Correspondence and requests for materials should be addressed to R.A.-L. or E.A.G.-V.

Reprints and permissions information is available at www.nature.com/reprints.

Publisher's note Springer Nature remains neutral with regard to jurisdictional claims in published maps and institutional affiliations.



Open Access This article is licensed under a Creative Commons Attribution 4.0 International License, which permits use, sharing, adaptation, distribution and reproduction in any medium or format, as long as you give appropriate credit to the original author(s) and the source, provide a link to the Creative Commons licence, and indicate if changes were made. The images or other third party material in this article are included in the article's Creative Commons licence, unless indicated otherwise in a credit line to the material. If material is not included in the article's Creative Commons licence and your intended use is not permitted by statutory regulation or exceeds the permitted use, you will need to obtain permission directly from the copyright holder. To view a copy of this licence, visit <http://creativecommons.org/licenses/by/4.0/>.

© The Author(s) 2024